High positive contrast generation of a subvoxel susceptibility deviation in ultrashort TE (UTE) radial center-out imaging at 3T

P. R. Seevinck[1], H. de Leeuw[1], C. Bos[2], and C. J. Bakker[1]

[1]Image Sciences Institute, Department of Radiology, University Medical Center, Utrecht, Utrecht, Netherlands, [2]Philips Healthcare Best, Best, Netherlands

Introduction- A number of positive contrast techniques for the detection of (super-) paramagnetic particles/agents, such as (U)SPIO or iron-oxide labeled cells have been developed recently. Most of these positive contrast (PC) techniques exploit the frequency shift that is induced by the magnetic susceptibility difference of the contrast agents. Positive contrast techniques may improve detectability (sensitivity) and/or specificity over conventional negative contrast techniques. In this work the artifact of a spherical subvoxel susceptibility deviation in 3D ultrashort TE (UTE) radial center-out imaging is investigated in the context of high positive contrast generation. Contrast to noise ratios (CNR) for UTE images are compared to CNR of conventional 3D images acquired with Cartesian and radial sampling schemes. Simulations are performed to investigate the influence of varying the size (volume) and strength ($\Delta\chi$,) of the susceptibility inclusion and the value of the read gradient on contrast generation in UTE.

Materials & Methods- Theory: The dipolar magnetic field perturbation of a sphere with susceptibility $\Delta\chi$ and radius a can be described by Eq. (1), in which B_0 is the field strength and r and θ designate spherical coordinates with respect to the sphere's center and B_0.

$$\Delta B(r,\theta) = \frac{\Delta\chi}{3}\left(\frac{a}{r}\right)^3 (3Cos^2\theta - 1)B_0 \quad [1]$$

$$S(t') = \sum_{n=0}^{N-1} \rho(n\cdot\Delta x)\cdot\exp\left(-i2\pi\gamma G_x^{im}\cdot t'\cdot(1+\frac{G_x^{sus}}{G_x^{im}})\cdot n\cdot\Delta x\right)\cdot\exp\left(-i2\pi\gamma G_x^{sus}\cdot TE\cdot n\cdot\Delta x\right) \quad [2]$$

$$k'(t') = \left(1+\frac{G_x^{sus}}{G_x^{im}}\right)\cdot k(t') \quad [3]$$

In a 1D FID experiment, the measured signal along the readout direction (x in Eq. 2 and 3) can be written in terms of t'(t'=t-TE) as shown Eq. [2] [1]. From Eq 2, we see that the locally induced magnetic field gradients influence the imaging experiment in two ways. Firstly, spatial encoding of spins is disturbed by the spatially varying susceptibility gradient (G^{sus}) during readout: in the first exponent the scaled k-space variable (k'(t')) can be identified, Eq. [3], which is independent of TE. This term causes the signal of spins to be spatially encoded with a frequency scaled according to $\lambda=1+(G^{sus}/G^{im})$, leading to a geometrical distortion. MR magnitude signal will be smeared out when $|\lambda|>1$ and piled up when $|\lambda|<1$. Since one k-space line is acquired using both positive and negative read gradients, the mis-mapping of frequencies will be symmetric with respect to the center of k-space. Secondly, an echo shift in k-space is induced since the susceptibility gradient acts locally in addition to the imaging gradients (G^{im}) and causes an unbalanced timing of the echo at TE. It is this echo shift that is responsible for T_2^* dephasing. The echo shift is represented by the second exponent (which leads to dephasing after integration over the voxel volume), which is negligible for ultrashort TE, so dephasing will not mask the geometrical distortions when using UTE. Simulations: Radial center-out k-space sampling was simulated in 1D on an axis perpendicular to B_0 to investigate the intensity profile of an object containing a spherical susceptibility inclusion. The dipolar magnetic field perturbation of the inclusion was calculated using Eq. (1) with $\Delta\chi$ = 4000ppm and a = 0.25 mm. A super-sampling factor of 10 was used to simulate possible dephasing. The R_2 of the object was set to R_2=30 s^{-1}. Other parameters included FOV = 128; imaging matrix = 256 and TE/ΔTE=0.08/2.3ms. G^{im} was set at 20 mT/m and 5 mT/m to investigate its influence. Finally, a cluster of 10000 iron-oxide labeled cells with a radius of 15 µm and $\Delta\chi$ = 1500 ppm was simulated to investigate a realistic $\Delta\chi$ inclusion. In vitro experiments: An iron spherical particle (radius a = 0.25mm) was submersed in an agarose gel (2%) phantom doped with 12 mg/ml MnCl to adapt R_2 (~30 s^{-1}). MR Imaging was done on a 3T system (Achieva, Philips Healthcare) with the following imaging parameters: FOV = 128mm; scan matrix = 128^3; reconstructed matrix = 256^3; NSA=1; flip = 8°, WFS = 0.5 pixels (=867Hz/pixel); G^{im} = 20mT/m. Timing parameters for 3D radial center-out UTE imaging were; TR/TE/ΔTE=16/0.08/2.3ms with 3 echoes, scan time ≈ 8 minutes for 26500 profiles. For conventional 3D radial imaging; TR/TE/ΔTE=11/1.98/2.3ms with 3 echoes, scan time ≈ 7 minutes. For conventional 3D imaging with Cartesian sampling TR/TE/ΔTE=11/1.81/2.3ms with 3 echoes, scan time ≈ 6 min. CNR values were calculated by determining the highest signal difference (ΔS) between positive and negative contrast divided by the standard deviation (sd) in the gel phantom: CNR= ΔS/sd.

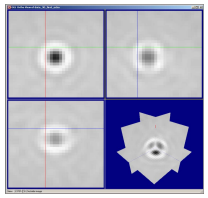

Fig. 1. Orthogonal views of a $\Delta\chi$ artifact in UTE imaging

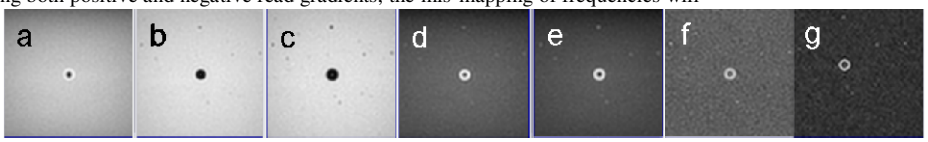

Figure 2. Transverse images (perpendicular to B_0) of UTE image (a), 2nd and 3rd echoes (b, c) and subtraction images of UTE minus 2nd (d), UTE minus 3rd (e),) and subtraction images (1st minus 3rd echo) acquired with 3D radial (f) and 3D cartesian (g) sampling.

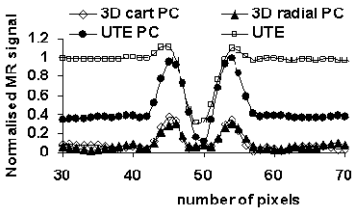

Figure 3. Intensity profiles of UTE and subtraction images of UTE, 3D radial and Cartesian sampling, normalized to UTE image.

Results- Signal pile-up around the iron sphere forms a spherical hyperintense artifact (Fig. 1) in center-out radial UTE imaging. In a transverse slice perpendicular to B_0, the hyperintense ring present at TE = 80 µsec (Fig. 2a) has disappeared at longer echo times (Fig. 2b, c), due to dephasing. PC was generated by subtracting a later echo from the UTE image (Fig. 2d,e) while suppressing long T_2[2], which is shown by the intensity profiles as well (Fig. 3). The CNR's (Table 1) of the UTE and subsequent echoes were similar. However, All CNR values of subtraction images from UTE imaging were substantially higher than the CNR's for conventional 3D radial (Fig. 3a, b) and Cartesian sampling (Fig. 3c, d). These differences cannot be explained by slight variations in total imaging time or TR which were similar for the three imaging methods. Simulation of center-out sampling of k-space showed similar intensity profiles as observed from experimental data (Fig. 3 and 4). Furthermore, lowering the imaging gradient resulted in a decrease of the signal pile up while broadening the artifact (Fig. 4e). Finally, the simulation shows that a cluster of 10000 iron-labeled cells (radius = 15 µm, $\Delta\chi$ = 1500 ppm) would induce a strong PC (Fig. 4f), suggesting the applicability of this method to be used for tracking of iron-labeled cells.

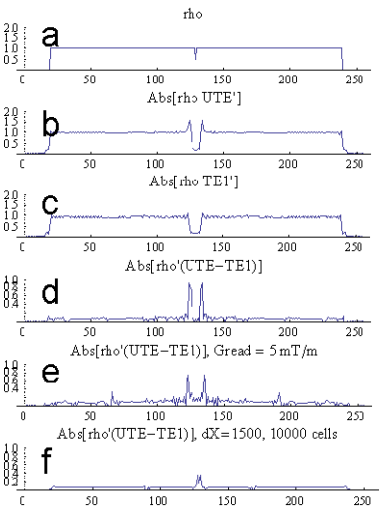

Fig. 4. 1D simulations of centered-out sampling of k-space. Object (a), UTE profile (b), 2nd echo (c), PC profile (d), influence of a low Gread (e) and simulation of a cluster of cells (f).

Discussion&Conclusion-UTE imaging can be used to generate high CNR positive contrast from susceptibility inhomogeneities. Increased CNR compared to conventional imaging methods with longer TE was observed, related to the lack of dephasing of the signal pile up created by the (super-) paramagnetic particle. Simulations have indicated that this imaging strategy may be well suitable for the detection of small amounts of (super-) paramagnetic substances.

Table 1.CNR's determined from 3D UTE, conventional radial and cartesian sampling of the $\Delta\chi$ marker.

Echo	UTE	Radial	Cart.
1st	52	47	49
2nd	56	30	38
3rd	55	28	36
1-2	47	16	16
1-3	61	22	19

[1] Dahnke H et al. MRM 2008;60:595-603

[2] Rahmer J et al. MAGMA 2007;20:83-92